First-order magnetic and structural phase transitions in Fe1+ySexTe1-x

S. L. Li, C. de la Cruz, Q. Huang, Y. Chen, J. W. Lynn, J. P. Hu, Y. L. Huang, F. C. Hsu, K. W. Yeh, M. K. Wu, and P. C. Dai

First-order magnetic and structural phase transitions in $Fe_{1+y}Se_xTe_{1-x}$

Shiliang Li,[1] Clarina de la Cruz,[1,2] Q. Huang,[3] Y. Chen,[3] J. W. Lynn,[3] Jiangping Hu,[4] Yi-Lin Huang,[5] Fong-Chi Hsu,[5] Kuo-Wei Yeh,[5] Maw-Kuen Wu,[5] and Pengcheng Dai[1,2]

[1]*Department of Physics and Astronomy, The University of Tennessee, Knoxville, Tennessee 37996-1200, USA*

[2]*Neutron Scattering Science Division, Oak Ridge National Laboratory, Oak Ridge, Tennessee 37831-6393, USA*

[3]*NIST Center for Neutron Research, National Institute of Standards and Technology, Gaithersburg, Maryland 20899, USA*

[4]*Department of Physics, Purdue University, West Lafayette, Indiana 47907, USA*

[5]*Institute of Physics, Academia Sinica, Nankang, Taipei, Taiwan*

(Received 2 November 2008; published 2 February 2009)

We use bulk magnetic susceptibility, electronic specific heat, and neutron scattering to study structural and magnetic phase transitions in $Fe_{1+y}Se_xTe_{1-x}$. $Fe_{1.068}Te$ exhibits a first-order phase transition near 67 K with a tetragonal-to-monoclinic structural transition and simultaneously develops a collinear antiferromagnetic (AF) order responsible for the entropy change across the transition. Systematic studies of the $FeSe_{1-x}Te_x$ system reveal that the AF structure and lattice distortion in these materials are different from those of FeAs-based pnictides. These results call into question the conclusions of present density-functional calculations, where $FeSe_{1-x}Te_x$ and FeAs-based pnictides are expected to have similar Fermi surfaces and therefore the same spin-density wave AF order.

DOI: 10.1103/PhysRevB.79.054503 PACS number(s): 74.70.Dd, 75.25.+z, 75.30.Fv, 75.50.Ee

I. INTRODUCTION

Superconductivity was recently discovered in the tetragonal-structured β phase (sometimes called α phase) $FeSe_x$ system[1–3] shortly after the discovery of high transition temperature superconductivity with T_c of up to 55 K in FeAs-based pnictides.[4–9] The T_c of the $Fe_{1+y}Se_xTe_{1-x}$ system can reach up to 14 K at ambient pressure[1,10–12] and 27 K at a pressure of 1.48 GPa.[13] Contrary to the earlier prediction of a low-T_c conventional superconductor,[14] density-functional calculations of the electronic structure, magnetism, and electron-phonon coupling for the superconducting phase of $Fe_{1+y}Se_xTe_{1-x}$ suggest that superconductivity in this class of materials is unconventional and mediated by spin fluctuations.[15] Furthermore, the calculated Fermi surface of $Fe_{1+y}Se_xTe_{1-x}$ is very similar to that of the iron pnictides such as LaFeAsO and $BaFe_2As_2$. If the observed collinear antiferromagnetic (AF) order in the parent compounds of the FeAs-based pnictides[16–23] is due to the spin-density wave (SDW) instability of a nested Fermi surface,[24–27] one would expect to find the same AF structure or SDW instability in the nonsuperconducting $Fe_{1+y}Se_xTe_{1-x}$. For FeAs-based materials such as $BaFe_2As_2$, $SrFe_2As_2$, and $CaFe_2As_2$, neutron-scattering experiments have shown that the system exhibits a tetragonal-to-orthorhombic lattice distortion accompanied by a collinear commensurate AF order with moment direction along the orthorhombic long (a) axis [Fig. 1(c)].[21–23] In the case of $Fe_{1+y}Se_xTe_{1-x}$, there have been several previous neutron and x-ray scattering experiments studying their structure and magnetic properties. More than 30 years ago, Fruchart *et al.*[28] discovered that $Fe_{1.125}Te$ orders antiferromagnetically with a commensurate structure at low temperature. Below the magnetic ordering temperature, these authors further showed that the crystal lattice exhibits a monoclinic distortion.[28] Recently, combined Rietveld refinements of the synchrotron x-ray and neutron powder-diffraction data on the superconducting $FeSe_{1-x}$ suggest that the crystal structure of

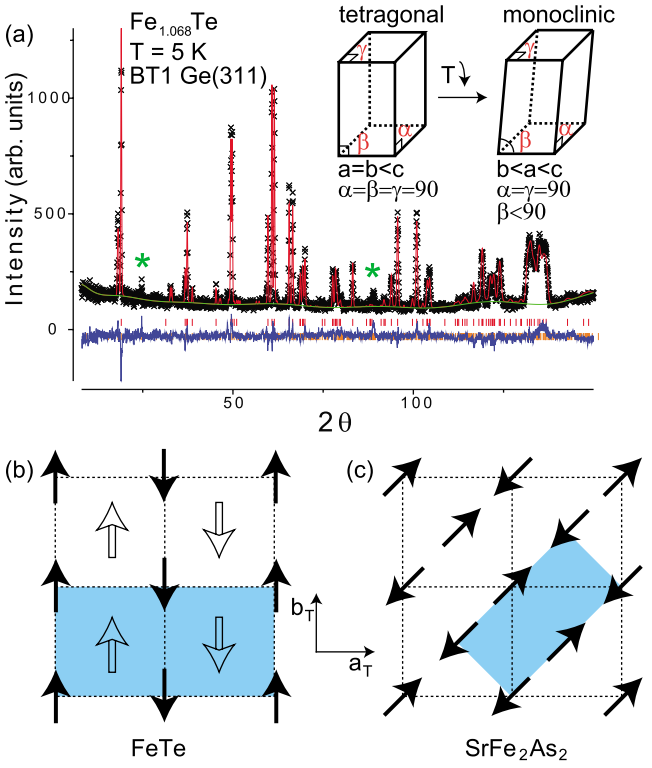

FIG. 1. (Color online) (a) Neutron powder-diffraction data of $Fe_{1.068}Te$ at $T=5$ K collected on the BT-1 diffractometer with Ge(3,1,1) monochromator and an incident-beam wavelength of $\lambda = 2.0785$ Å. The lattice structure is described by the monoclinic space group $P2_1/m$, which changes to tetragonal $P4/nmm$ above T_N, as illustrated schematically in the inset. (b) Schematic in-plane spin structure of $Fe_{1.068}Te$. The solid arrows and hollow arrows represent two sublattices of spins, which can be either parallel or antiparallel, as discussed in the text. The shaded area indicates the magnetic unit cell. (c) Schematic in-plane spin structure of $SrFe_2As_2$ from Ref. 22.

the material exhibits a tetragonal-to-orthorhombic phase transition near 70 K, displaying an identical distortion of the FeSe layers to that of the LaFeAsO.[11] Finally, Bao *et al.*[29] (in a very recent preprint) reported systematic neutron-scattering studies of the $Fe(Te_{1-x}Se_x)$ systems and found a low-temperature incommensurate AF order for $Fe_{1.141}Te$ with orthorhombic lattice distortion. The incommensurability decreases with decreasing Fe and the system locks into the commensurate AF structure for $Fe_{1.1076}Te$ with a monoclinic lattice distortion similar to a previous work on $Fe_{1.125}Te$.[28] When the long-range static AF order is suppressed by substitution of Te with Se, superconductivity appears and the incommensurate AF order with the in-plane propagation wave-vector $(\delta\pi, \delta\pi)$ direction (along the diagonal direction of the Fe-Fe square) becomes short-range spin fluctuations.[29] Based on these results, the authors argued that incommensurate AF interactions offer an alternative possibility for mediating electron pairing for superconductivity in $Fe(Te_{1-x}Se_x)$,[29] and therefore fundamentally different from FeAs-based materials, where AF spin order in their parent compounds has commensurate AF propagation wave vector $(\pi,0)$ along the *a*-axis direction with an orthorhombic lattice structure.[16–23]

To understand this apparent discrepancy in the AF structures of these two systems, we carried out systematic neutron-scattering studies of the $Fe_{1+y}Te$ system. We show that there are excess magnetic Fe ions in $Fe_{1+y}Te$ sitting in the octahedral sites.[28,30,31] Although stoichiometric FeTe is difficult to synthesize,[30] the Fe spins in $Fe_{1.068}Te$ form a collinear commensurate AF structure with moments confined within the *a*-*b* plane of the monoclinic structure as shown in Fig. 1(b). Consistent with earlier measurements,[32,33] we find that the AF phase transition is of the first order with an entropy change of ~ 3.2 J/(mol K). Systematic studies of $FeSe_{0.416}Te_{0.584}$ and $FeSe_{0.493}Te_{0.507}$ reveal that the differences in lattice distortions between $FeSe_{1-x}Te_x$ and LaFeAsO can account for the differences in their magnetic structures. These results are difficult to explain within the previous density-functional calculations, where FeTe, FeSe, and LaFeAsO are expected to have similar Fermi surfaces and therefore similar SDW-like AF order.[15] However, more recent density-functional calculations suggest that the excess Fe in $Fe_{1+y}Te$ is strongly magnetic and is also an electron donor.[34] The excess magnetic Fe might account for the observed differences in magnetic structures of $Fe_{1+y}Te$ and other FeAs-based pnictides.

II. EXPERIMENTAL RESULTS AND DISCUSSIONS

We prepared powder samples of $Fe_{1+y}Se_xTe_{1-x}$ with nominal composition of $x=0$, 0.3, and 0.5 using the method described elsewhere.[10] $Fe_{1+y}Te$ is nonsuperconducting while the other two samples have T_c of ~ 14 K.[10,12] Powder neutron-diffraction data were taken on the BT-1 powder diffractometer at the NIST Center for Neutron Research (NCNR), Gaithersburg, Maryland. The BT-1 diffractometer has a Ge(3,1,1) monochromator which was set to have an incident wavelength of $\lambda=2.0785$ Å. Collimators with horizontal divergences of 15′, 20′, and 7′ full width at half maximum (FWHM) were used before and after the monochromator, and after the sample, respectively. For structural analysis, we use the BT-1 powder diffractometer because of its high wave-vector Q resolution. For studying weak magnetic peaks, we employ the high-flux BT-7 triple-axis spectrometer with a pyrolytic graphite [PG(0,0,2)] monochromator and incident-beam wavelength of $\lambda=2.359$ Å. A PG filter was placed in the incident-beam path to eliminate $\lambda/2$. The collimations are 50′ before the sample and 80′ radial between the sample and a position sensitive detector that covered an angular range of approximately 5°. The sample was loaded inside the helium-gas-filled sample chamber in a top-loading closed cycle refrigerator (CCR). We define the nuclear wave vector Q at (q_x,q_y,q_z) as $(H,K,L)=(q_xa/2\pi, q_yb/2\pi, q_zc/2\pi)$ reciprocal-lattice units (rlu) in both the tetragonal and monoclinic unit cells. We used a commercial superconducting quantum interference device (SQUID) and a physical property measurement system (PPMS) to measure the dc susceptibility and specific heat of the samples used for neutron measurements.

We first discuss nuclear and magnetic structures of the nonsuperconducting $Fe_{1+y}Te$. For the initial Rietveld refinement using BT-1 powder-diffraction data, the Te content was assumed to be 1 since previous work has found that FeTe and FeSe tend to be Fe rich.[29,35] At 80 K, $Fe_{1+y}Te$ has a tetragonal crystal structure with space group $P4/nmm$ and no static magnetic order. Our Rietveld analysis reveals that the system actually has excess Fe with $y=0.068(3)$. On cooling to 5 K, the nuclear structure changes to monoclinic with the space group $P2_1/m$, as confirmed by the splitting of the (1,1,2) nuclear Bragg peak to $(1,1,2)/(1,1,-2)$ peaks from 80 to 40 K shown in the inset of Fig. 1(a) and refinement results in Table I. An orthorhombic lattice distortion similar to that in FeAs-based materials[16–23] and in $Fe_{1.141}Te$ should split the (2,0,0) Bragg peak, leaving the (1,1,2) reflection unchanged as discussed in Ref. 29. In addition to confirming the monoclinic structure, the outcome of the refinements revealed excess Fe in the nonsuperconducting $Fe_{1+y}Te$. Since the Fe(1) occupancy is very close to 1, the total Fe content in $Fe_{1+y}Te$ is labeled as 1.068 to reflect the excess Fe. The observed low-temperature monoclinic lattice distortion in $Fe_{1.068}Te$ is consistent with previous results on $Fe_{1.125}Te$ (Ref. 28) and $Fe_{1.076}Te$.[29] For oxypinctides such as LaFeAsO and CeFeAsO, the lattice distortion changes the symmetry from tetragonal to orthorhombic.[16,17] In the case of $Fe_{1+y}Te$, the lattice distortion is from tetragonal to monoclinic with the β angle between *a* and *c* axes being reduced to less than 90° while the nearest Fe-Fe distance remains unchanged (see Table I).

Figure 1(c) shows the schematic in-plane spin structure of $SrFe_2As_2$, where the Fe moments form a collinear AF structure with spin directions along the *a* axis (the long axis) of the orthorhombic structure. This magnetic structure appears to be ubiquitous for parent compounds of FeAs-based superconductors.[16–23] To see if the magnetic structure of $Fe_{1.068}Te$ is consistent with that of $Fe_{1.125}Te$ (Ref. 28) and $Fe_{1.076}Te$,[29] we initially fix the moment direction within the Fe-Fe layer and choose the $P1$ space group for the Fe(1) position in the GSAS program to refine the magnetic structure using the method described in Ref. 36. Consistent with ear-

TABLE I. Refinement of powder-diffraction data.

$Fe_{1.068}Te(5\ K)$, $P2_1/m$, $\chi^2=1.559$, $\beta=89.212(3)°$					
$a=3.834\ 47(19)(Å)$, $b=3.784\ 14(18)(Å)$, $c=6.257\ 18(30)(Å)$					
Atom	Site	x	y	z	Occupancy
Fe(1)	2*b*	0.75	0.25	0.0035(7)	0.995[a]
Te	2*a*	0.25	0.25	0.2798(6)	1[b]
Fe(2)	2*a*	0.25	0.25	0.6812(5)	0.068[a]
$Fe_{1.068}Te(80\ K)$, $P4/nmm$, $\chi^2=1.387$					
$a=3.812\ 34(8)(Å)$, $b=3.812\ 34(8)(Å)$, $c=6.2517(2),(Å)$					
Atom	Site	x	y	z	Occupancy
Fe(1)	2*b*	0.75	0.25	0	0.995(11)
Te	2*a*	0.25	0.25	0.2829(4)	1[b]
Fe(2)	2*a*	0.25	0.25	0.7351(3)	0.068(3)
$FeSe_{0.416}Te_{0.584}(10\ K)$, $P4/nmm$, $\chi^2=2.588$					
$a=3.802\ 87(8)(Å)$, $b=3.802\ 87(8)(Å)$, $c=6.083\ 49(18)(Å)$					
Atom	Site	x	y	z	Occupancy
Fe(1)	2*b*	0.75	0.25	0	1[c]
Se	2*a*	0.25	0.25	0.2708(4)	0.416(23)[d]
Te	2*a*	0.25	0.25	0.2708(4)	0.584(23)[d]
Fe(2)	2*a*	0.25	0.25	0.6690(26)	0.088(4)
$FeSe_{0.493}Te_{0.507}(5\ K)$, $P4/nmm$, $\chi^2=2.754$					
$a=3.793\ 27(9)(Å)$, $b=3.793\ 27(9)(Å)$, $c=5.955\ 19(21)(Å)$					
Atom	Site	x	y	z	Occupancy
Fe	2*b*	0.75	0.25	0	1[c]
Se	2*a*	0.25	0.25	0.2719(5)	0.493(24)[d]
Te	2*a*	0.25	0.25	0.2719(5)	0.507(24)[d]
Fe(2)	2*a*	0.25	0.25	0.643(5)	0.054(5)

[a]Fe(1) and Fe(2) occupancies are fixed as the values determined at 80 K.
[b]Te occupancy is fixed to 1.
[c]Fe occupancy is fixed to 1.
[d]The sum of Se and Te is constrained to be 1.

lier results,[28,29] we find that an approximate magnetic structure, as shown in Fig. 1(b), can describe the observed magnetic peaks reasonably well. To further refine the magnetic structure, we relaxed the constraints of moment along both *a* and *c* directions and carried out the Rietveld analysis. The Fe has a total moment of $2.25(8)\mu_B$/Fe with a majority of the moment $[2.0(7)\mu_B/\mathrm{Fe}]$ along the *b*-axis direction. Our refinement on $Fe_{1.068}Te$ reveals that the spin structure in this system is also collinear with a major component of the moment along the tetragonal *b* axis as shown in Fig. 1(b). This result is consistent with previous work on $Fe_{1.125}Te$ (Ref. 28) and $Fe_{1.076}Te$,[29] and thus suggests that incommensurate magnetic order found in $Fe_{1.141}Te$ locks into commensurate AF order with decreasing Fe concentration very rapidly. We cannot determine whether the direction of the corner spin at the (0,0) position is parallel or antiparallel to that of the center spin at (0.5,0.5) in Fig. 1(b) since the absolute values of the structure factors for these two configurations are very close in a slightly distorted monoclinic structure. However, the in-plane spin directions in $Fe_{1.068}Te$ are rotated 45° from those in the Fe-As materials. This is different from the prediction of the density-functional calculations,[15] where Fermi surfaces of these two materials, and therefore the spin-density wave instability due to nested Fermi surfaces, are expected to be very similar.

In addition to the large moment ($\sim 2.0\mu_B$/Fe) along the tetragonal *b*-axis direction, we find that the projections of the moment along the *a* and *c* axes are $-0.7(2)\mu_B$ and $0.7(1)\mu_B$, respectively. For FeAs-based materials, the static ordered moments are strictly within the *a*-*b* plane of the crystalline unit cell.[16–23] We speculate that the finite moments along the *c*-axis direction in $Fe_{1.068}Te$ are due to the finite moments of the excess Fe ions.[34] Although the total moment of the $Fe_{1.068}Te$ per Fe ion is similar to that in $Fe_{1.125}Te$,[28] the *c*-axis component of the moment in $Fe_{1.125}Te$ is $1.36\mu_B$.[28] This difference may be related to the amount of excess Fe ions in the octahedral site,[28,30,31] which is expected to be strongly magnetic.[34] Since the moments of the excess Fe ions

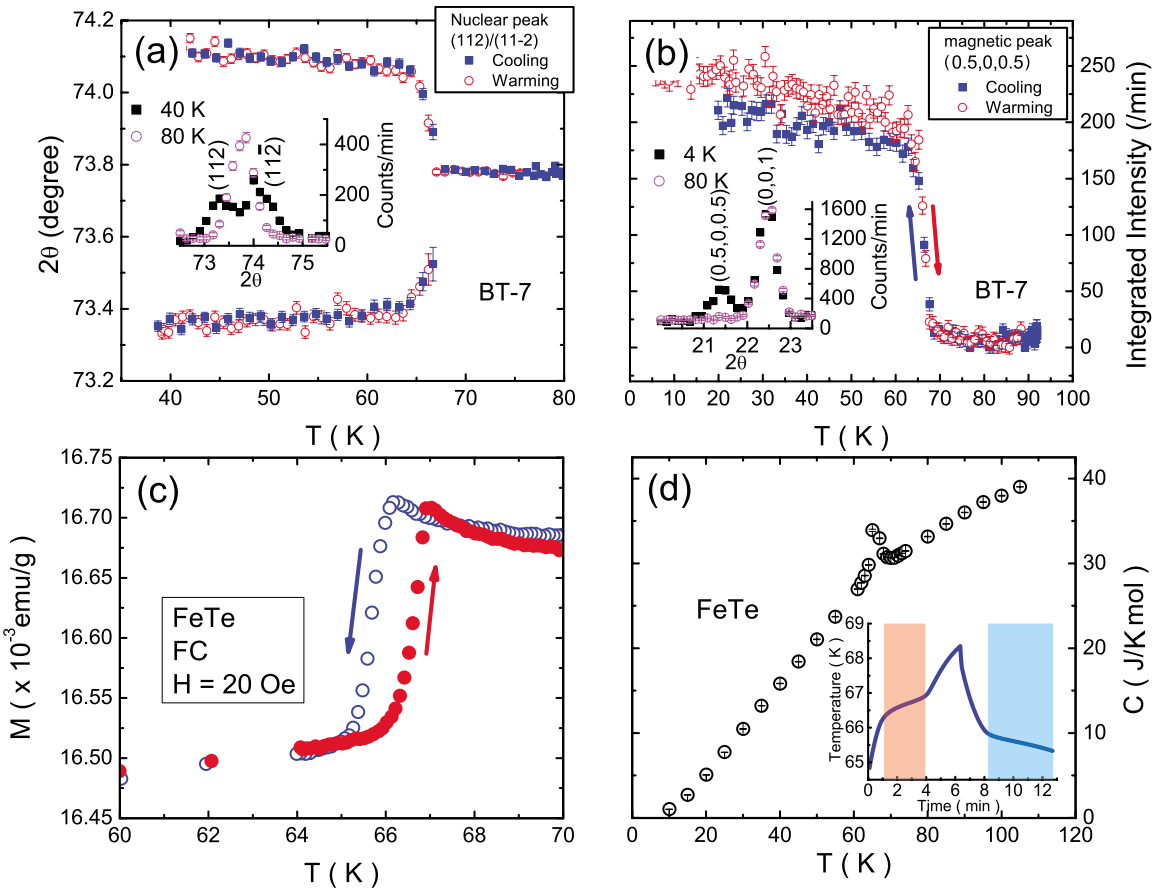

FIG. 2. (Color online) (a) Splitting of the (1,1,2) and (1,1,−2) nuclear peaks with decreasing temperature due to the tetragonal-monoclinic lattice distortion. (b) Temperature dependence of the (0.5,0,0.5) AF Bragg peak indicates a strong coupling to the structural distortion. (c) dc magnetic susceptibility measured by SQUID shows a temperature hysteresis of about 1 K. (d) Specific-heat measurements show a sharp peak around the structural/magnetic phase transition. The inset shows the raw data of the thermal-relaxation calorimeter of the PPMS, where the plateaus during warming and cooling processes clearly reveal the absorption and liberation of the latent heat.

are randomly distributed between the Fe-Fe layers, the Fe moments in $Fe_{1.125}Te$ tend to cant toward the c axis. However, the random nature of the excess Fe ions makes it very difficult to estimate their moment sizes and determine their influence to the in-plane Fe AF spin structure using the conventional neutron diffraction described here because such a technique is insensitive to a disordered lattice. Assuming that the incommensurate AF order observed for $Fe_{1.141}Te$ (Ref. 29) indeed arises from the magnetic interactions between the in-plane Fe and the large excess magnetic Fe ions in the octahedral site, the reduction in the excess Fe should then drive the system toward the stoichiometric FeTe and decrease the influence of the excess Fe. This in turn favors the commensurate AF spin structure shown in Fig. 1(b). If this picture is correct, the incommensurate AF order in $Fe_{1.141}Te$ (Ref. 29) should not be a fundamental property of the stoichiometric FeTe.

To understand the nuclear and magnetic phase transitions of $Fe_{1.068}Te$, we focus on the (1,1,2)/(1,1,−2) nuclear and (0.5,0,0.5) magnetic Bragg peaks. As shown in the inset of Fig. 2(a), the (1,1,2)/(1,1,−2) reflections split into two peaks due to the tetragonal-monoclinic structural transition. By fitting with one and two Gaussian peaks at high and low temperatures, respectively, we find that the structural phase transition happens near 67 K. Figure 2(b) shows that the temperature dependence of the (0.5,0,0.5) magnetic peak is clearly associated with the structural phase transition. In addition, the FWHM of the (0.5,0,0.5) peak is larger than the resolution due to the splitting of the (0.5,0,0.5) and (0.5,0,−0.5) peaks. We note that Ref. 29 also presented similar measurements on $Fe_{1.141}Te$ with a large (about 10 K) hysteresis using a conventional vacuum pumped displex refrigerator on BT-1. When we used the same CCR, we obtained similarly large hysteresis on $Fe_{1.068}Te$. However, since we cannot reproduce such a large hysteresis when the same sample is mounted in a He-gas-filled top-loading CCR, we believe that the initially observed large hysteresis in the $Fe_{1.068}Te$ is not an intrinsic property of the material but arises from poor thermal contact in the vacuum pumped bottom-loading CCR.[37]

To see if the 67 K phase transition is of the first or second order, we measured the magnetic susceptibility using a SQUID. Figure 2(c) shows that the dc susceptibility with field-cooled (FC) process and an applied magnetic field of 20 Oe has a clear hysteresis (about 1 K) near the structural/magnetic phase transitions. The first-order nature of the structural/magnetic phase transitions is shown unambiguously in the heat-capacity measurement. Similar to the pre-

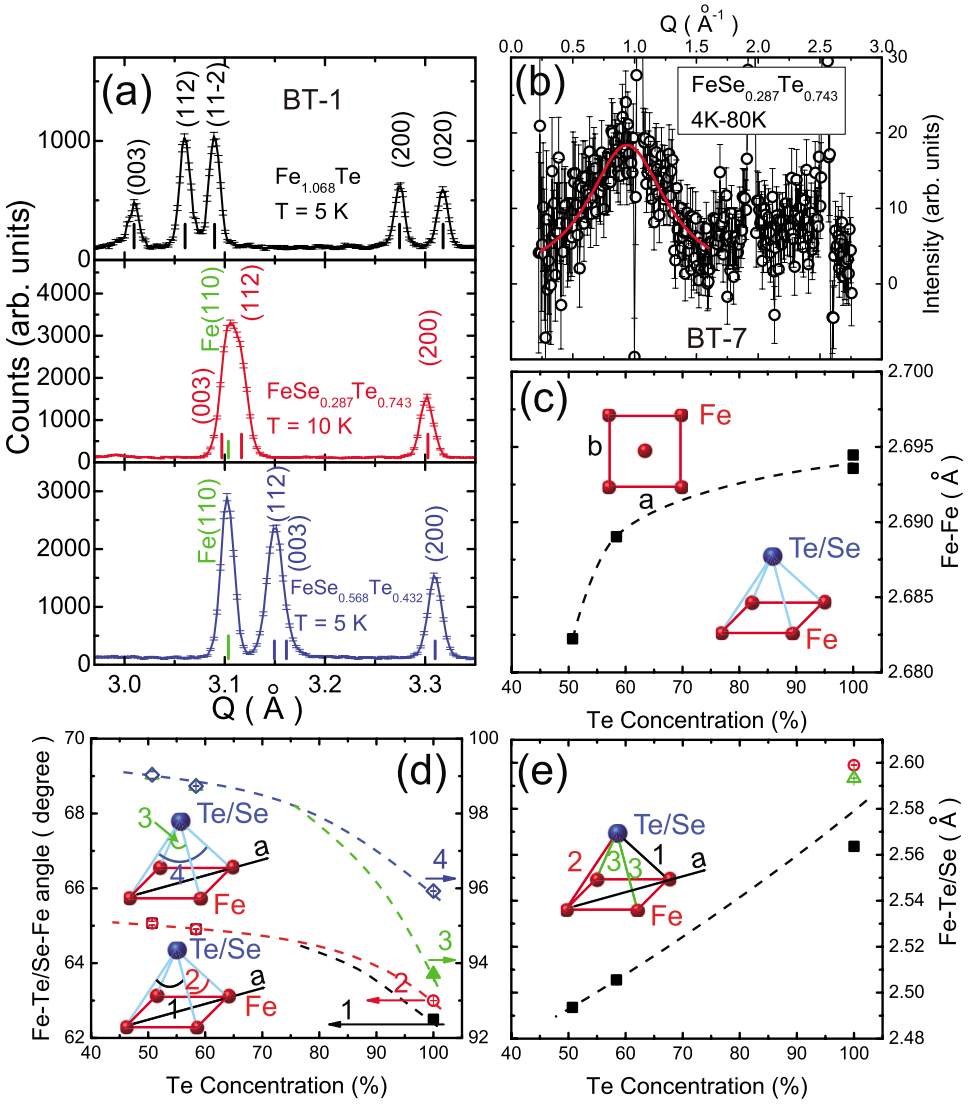

FIG. 3. (Color online) (a) Evolution of the (1,1,2)/(1,1,−2) and (2,0,0)/(0,2,0) peaks at low temperatures in $Fe_{1.068}Te$, $FeSe_{0.416}Te_{0.584}$, and $FeSe_{0.493}Te_{0.503}$. (b) Short-range AF fluctuations at Q=0.938 Å^{-1} with FWHM=0.67 Å^{-1} in $FeSe_{0.416}Te_{0.584}$. (c)–(e) show the doping dependence of nearest-neighbor Fe-Fe distance, the angles of Fe-Te/Se-Fe, and Fe-Te/Se distances, respectively.

vious study in $Fe_{1.11}Te$,[33] a sharp peak is found around the phase-transition temperature [Fig. 2(d)]. The heat-capacity option of the PPMS does not work accurately in the vicinity of the first-order transition.[38] To overcome this problem, we set the "temperature rise" option of the PPMS heat-capacity measurement to be 3 K and recorded the raw data of the calorimeter. Without the phase transition, the sample temperature increases and decreases smoothly during the heating and cooling processes, respectively. Around 67 K, however, plateaus due to the heat absorption and liberation from the first-order phase transition become apparent, as shown in the inset of Fig. 2(d). Based on these data and a fixed heating power of 0.286 mW, we estimate that the latent heat of the phase transition is ~215 J/mol, assuming it is supplied by the heat during the time of plateau in the heating process. This value gives a change in entropy of ΔS ~3.2 J/(mol K) through the transition. If we assume that the local Fe moment in FeTe is about 3.87μ_B in the paramagnetic state[39] and 1.7μ_B below T_N, the change in the entropy across the transition based on an Ising model is about 3.5 J/(mol K). These results suggest that the major contribution to the entropy change at the phase transition can be provided by the AF transition, which favors the view that the first-order phase transition is driven by the magnetism.[40]

Finally, we discuss the lattice distortions and magnetic structure in $Fe_{1+y}Se_{1-x}Te_x$ as superconductivity is induced by replacing Te with Se.[10,12] Although we find no static long-range-ordered magnetic Bragg peaks in the superconducting $FeSe_{0.416}Te_{0.584}$ and $FeSe_{0.493}Te_{0.507}$ samples similar to the Fe-As-based materials,[16,17] short-range spin fluctuations with correlation length of 9.4 Å were found in $FeSe_{0.416}Te_{0.584}$ at Q=0.938 Å^{-1} as shown in Fig. 3(b). The Q value is slightly less than the Q value of 0.974 Å^{-1} at the commensurate position (0.5,0,0.5). Since our $Fe_{1+y}Se_xTe_{1-x}$ samples do not exhibit incommensurate AF order, we believe that the observed small wave-vector deviation from the commensurate position in $FeSe_{0.416}Te_{0.584}$ is due to the variation in the magnetic form factor as well as a possible variation in the magnetic structure factor. However, one has to be vigilant for impurity phases as well.[39,41] For example, we can clearly see the strong (1,1,0) cubic Fe impurity peaks in Fig. 3(a) in both superconducting samples, which suggests the nonstoichiometry of our samples and the possible existence of other phases. Reference 29 also reported short-range spin fluctua-

tions in superconducting $Fe_{1.08}Te_{0.67}Se_{0.33}$, which centers at $Q=0.895$ Å^{-1}. The authors suggested a possible explanation for spin-spin correlations based on incommensurate magnetic peaks.[29] However, we believe that this is unlikely to be the case in our superconducting $Fe_{1+y}Se_xTe_{1-x}$, although we cannot rule this out.

Figure 3 and Table I summarize the doping evolution of some structural parameters for $Fe_{1+y}Se_{1-x}Te_x$. In the refinement of the superconducting samples, the Fe(1) composition and the sum of Se and Te are constrained to be 1. The Fe-Te distance increases approximately linearly with increasing Te concentration, as shown in Fig. 3(e). On the other hand, the Fe-Te/Se-Fe angles [Fig. 3(d)] decrease with increasing Te concentration. For $Fe_{1.068}Te$, the Fe-Te/Se-Fe angle along the *b* axis is much smaller than that along the *a* axis. Because of the low-temperature monoclinic structure, the perfect Fe-Te/Se tetrahedron is distorted, resulting in different Fe-Te/Se-Fe angles between the nearest Fe ions. We labeled these angles as 1 and 2 in Fig. 3(d). This distortion of the Fe-Te/Se tetrahedron is also illustrated by the Fe-Te/Se distances in $Fe_{1.068}Te$ [Fig. 3(e)].

To put these results in a proper context, we note that the density-functional calculations predicted a similar Fermi surface for $Fe_{1+y}Te$- and FeAs-based materials.[15] Therefore, within the itinerant electron picture, where the observed AF order in these two classes of materials arises from the same Fermi-surface nesting, one should expect a similar SDW instability or AF spin structure. Although experimentally we have observed different magnetic structures for the $Fe_{1+y}Te$ and LaFeAsO families of materials, the possible presence of a large magnetic moment on the excess Fe ion in between the ordered Fe layers in $Fe_{1+y}Te$ might influence the in-plane magnetic structure and resolve this inconsistency.[34] Alternatively, a model based on the localized magnetic exchange interactions can well explain the experimental results.[42] In fact, the difference between the Fe-Te/Se-Fe angles along the *a* and *b* axes should result in different next-nearest-neighbor couplings J_{2a} and J_{2b} that are responsible for the observed collinear AF structure. The difference between angles 1 and 2 due to the monoclinic lattice distortion may give rise to different nearest-neighbor couplings J_{1a} and J_{1b}. This could in turn stabilize the proposed spin structure in Fig. 1(b) where a spin is actually frustrated by the four nearest spins in a perfect rectangle.[43] Future experiments on stoichiometric FeTe samples should be able to conclusively determine whether the observed commensurate magnetic structure is a consequence of the excess Fe magnetic ions.

III. CONCLUSIONS

In conclusion, we have systematically studied the structural and magnetic phase transitions in the α-phase $Fe_{1+y}Se_xTe_{1-x}$ system. In the pure $Fe_{1+y}Te$, we find that structural and magnetic phase transitions are intimately connected and are first order in nature. The spin structure in $Fe_{1+y}Te$ is different from all other FeAs-based parent materials. Our results show the possible important role played by the excess Fe ions in determining the magnetic structure of $Fe_{1+y}Te$ and suggest that the magnetic ordering can provide enough energy for driving the first-order phase transition.

ACKNOWLEDGMENTS

We thank David Singh for helpful discussions. This work was supported by the U.S. NSF under Grants No. DMR-0756568 and No. PHY-0603759, by the BES, U.S. DOE through Grant No. DE-FG02-05ER46202, and Division of Scientific User Facilities.

[1] F.-C. Hsu *et al.*, Proc. Natl. Acad. Sci. U.S.A. **105**, 14262 (2008).
[2] W. Schuster, H. Mikler, and K. L. Komarek, Monatsh. Chem. **110**, 1153 (1979).
[3] H. Okamoto, J. Phase Equilib. **12**, 383 (1991).
[4] Y. Kamihara, T. Watanabe, M. Hirano, and H. Hosono, J. Am. Chem. Soc. **130**, 3296 (2008).
[5] X. H. Chen, T. Wu, G. Wu, R. H. Liu, H. Chen, and D. F. Fang, Nature (London) **453**, 761 (2008).
[6] G. F. Chen, Z. Li, D. Wu, G. Li, W. Z. Hu, J. Dong, P. Zheng, J. L. Luo, and N. L. Wang, Phys. Rev. Lett. **100**, 247002 (2008).
[7] Z.-A. Ren *et al.*, Europhys. Lett. **83**, 17002 (2008).
[8] M. Rotter, M. Tegel, and D. Johrendt, Phys. Rev. Lett. **101**, 107006 (2008).
[9] H. H. Wen, G. Mu, L. Fang, H. Yang, and X. Zhu, Europhys. Lett. **82**, 17009 (2008).
[10] K.-W. Yeh, T.-W. Huang, Y.-L. Huang, T.-K. Chen, F.-C. Hsu, P. M. Wu, Y.-C. Lee, Y.-Y. Chu, C.-L. Chen, J.-Y. Luo, D. C. Yan, and M. K. Wu, Europhys. Lett. **84**, 37002 (2008).
[11] S. Margadonna, Y. Takabayashi, M. T. McDonald, K. Kasperkiewicz, Y. Mizuguchi, Y. Takano, A. N. Fitch, E. Suard, and K. Prassides, Chem. Commun. (Cambridge) (2008) 5607.
[12] M. H. Fang, H. M. Pham, B. Qian, T. J. Liu, E. K. Vehstedt, Y. Liu, L. Spinu, and Z. Q. Mao, Phys. Rev. B **78**, 224503 (2008).
[13] Y. Mizuguchi, F. Tomioka, S. Tsuda, T. Yamaguchi, and Y. Takano, Appl. Phys. Lett. **93**, 152505 (2008).
[14] S. Atzeri and G. Mula, Solid State Commun. **13**, 157 (1973).
[15] A. Subedi, L. Zhang, D. J. Singh, and M. H. Du, Phys. Rev. B **78**, 134514 (2008).
[16] C. de la Cruz, Q. Huang, J. W. Lynn, J. Li, W. Ratcliff, J. L. Zarestky, H. A. Mook, G. F. Chen, J. L. Luo, N. L. Wang, and Pengcheng Dai, Nature (London) **453**, 899 (2008).
[17] J. Zhao, Q. Huang, C. de la Cruz, S. Li, J. W. Lynn, Y. Chen, M. A. Green, G. F. Chen, G. Li, Z. Li, J. L. Luo, N. L. Wang, and Pengcheng Dai, Nature Mater. **7**, 953 (2008).
[18] Y. Chen, J. W. Lynn, J. Li, G. Li, G. F. Chen, J. L. Luo, N. L. Wang, Pengcheng Dai, C. dela Cruz, and H. A. Mook, Phys. Rev. B **78**, 064515 (2008).
[19] S. A. J. Kimber, D. N. Argyriou, F. Yokaichiya, K. Habicht, S. Gerischer, T. Hansen, T. Chatterji, R. Klingeler, C. Hess, G. Behr, A. Kondrat, and B. Buchner, Phys. Rev. B **78**, 140503(R) (2008).

[20] J. Zhao, Q. Huang, C. de la Cruz, J. W. Lynn, M. D. Lumsden, Z. A. Ren, Jie Yang, Xiaolin Shen, Xiaoli Dong, Zhongxian Zhao, and Pengcheng Dai, Phys. Rev. B **78**, 132504 (2008).
[21] Q. Huang, Y. Qiu, W. Bao, M. A. Green, J. W. Lynn, Y. C. Gasparovic, T. Wu, G. Wu, and X. H. Chen, Phys. Rev. Lett. **101**, 257003 (2008).
[22] J. Zhao, W. Ratcliff, J. W. Lynn, G. F. Chen, J. L. Luo, N. L. Wang, J. Hu, and P. Dai, Phys. Rev. B **78**, 140504(R) (2008).
[23] A. I. Goldman, D. N. Argyriou, B. Ouladdiaf, T. Chatterji, A. Kreyssig, S. Nandi, N. Ni, S. L. Bud'ko, P. C. Canfield, and R. J. McQueeney, Phys. Rev. B **78**, 100506(R) (2008).
[24] Z. P. Yin, S. Lebègue, M. J. Han, B. P. Neal, S. Y. Savrasov, and W. E. Pickett, Phys. Rev. Lett. **101**, 047001 (2008).
[25] I. I. Mazin, D. J. Singh, M. D. Johannes, and M. H. Du, Phys. Rev. Lett. **101**, 057003 (2008).
[26] J. Dong *et al.*, Europhys. Lett. **83**, 27006 (2008).
[27] F. Ma, Z.-Y. Lu, and T. Xiang, Phys. Rev. B **78**, 224517 (2008).
[28] D. Fruchart, P. Convert, P. Wolfers, R. Madar, J. P. Senateur, and R. Fruchart, Mater. Res. Bull. **10**, 169 (1975).
[29] W. Bao *et al.*, arXiv:0809.2058 (unpublished).
[30] F. Grønvold, H. Haraldsen, and J. Vihovde, Acta Chem. Scand. (1947-1973) **8**, 1927 (1954).
[31] J. B. Ward and V. H. McCann, J. Phys. C **12**, 873 (1979).
[32] I. Tsubokawa and S. Chiba, J. Phys. Soc. Jpn. **14**, 1120 (1945).
[33] E. F. Westrum, C. Chou, and F. Grφnvold, J. Chem. Phys. **30**, 761 (1959).
[34] L. Zhang, D. J. Singh, and M. H. Du, arXiv:0810.3274, Phys. Rev. B (to be published).
[35] T. M. McQueen, Q. Huang, V. Ksenofontov, C. Felser, Q. Xu, H. Zandbergen, Y. S. Hor, J. Allred, A. J. Williams, D. Qu, J. Checkelsky, N. P. Ong, and R. J. Cava, arXiv:0811.1613, Phys. Rev. B (to be published).
[36] J. Cui, Q. Huang, and B. H. Toby, Powder Diffr. **21**, 71 (2006).
[37] Q. Huang (private communication).
[38] J. C. Lashley *et al.*, Cryogenics **43**, 369 (2003).
[39] K. L. Komarek and P. Terzieff, Monatsh. Chem. **106**, 145 (1975).
[40] C. Fang, H. Yao, W. F. Tsai, J. P. Hu, and S. A. Kivelson, Phys. Rev. B **77**, 224509 (2008).
[41] P. Terzieff, Physica B & C **103**, 158 (1981).
[42] F. Ma, W. Ji, J. Hu, Z.-Y. Lu, and T. Xiang, arXiv:0809.4732 (unpublished).
[43] C. Fang, B. A. Bernevig, and J. Hu, arXiv:0811.1294 (unpublished).